Available online at www.sciencedirect.com
ScienceDirect
C. R. Physique 10 (2009) 849–858
COMPTES RENDUS PHYSIQUE

Experimental determination of Boltzmann's constant

Electronic measurement of the Boltzmann constant with a quantum-voltage-calibrated Johnson noise thermometer ☆

Samuel Benz [a,*], D. Rod White [b], JiFeng Qu [a], Horst Rogalla [c], Weston Tew [d]

[a] *National Institute of Standards and Technology, 325 Broadway, Boulder, CO 80305, USA*
[b] *Measurement Standards Laboratory, P.O. Box 31310, Lower Hutt 5040, New Zealand*
[c] *Department of Applied Physics, Univ. Twente, P.O. Box 217, 7500 AE Enschede, The Netherlands*
[d] *National Institute of Standards and Technology, Gaithersburg, MD 20899, USA*

Available online 22 November 2009

Abstract

Currently, the CODATA value of the Boltzmann constant is dominated by a single gas-based thermometry measurement with a relative standard uncertainty of 1.8×10^{-6} [P.J. Mohr, B.N. Taylor, D.B. Newell, CODATA recommended values of the fundamental physical constants: 2006, Rev. Mod. Phys. 80 (2008) 633–730]. This article describes an electronic approach to measuring the Boltzmann constant that compares Johnson noise from a resistor at the water triple point with a pseudo-random noise generated using quantized ac-voltage synthesis. Measurement of the ratio of the two power spectral densities links Boltzmann's constant to Planck's constant. Recent experiments and detailed uncertainty analysis indicate that Boltzmann's constant can presently be determined using Johnson noise with a relative standard uncertainty below 10×10^{-6}, which would support both historic and new determinations. ***To cite this article: S. Benz et al., C. R. Physique 10 (2009).***

Résumé

Mesures de la constante de Boltzmann à l'aide d'un thermomètre résistif à bruit Johnson étalonné par une source de tension quantique. La valeur de la constante de Boltzmann recommandée par CODATA résulte presque uniquement de mesures obtenues par thermométrie à gaz avec une incertitude relative de 1.8×10^{-6} [P.J. Mohr, B.N. Taylor, D.B. Newell, CODATA recommended values of the fundamental physical constants: 2006, Rev. Mod. Phys. 80 (2008) 633–730]. Cet article présente une mesure électrique de la constante de Boltzmann effectuée en comparant le bruit Johnson d'une résistance placée à la température du point triple de l'eau avec un signal pseudo aléatoire généré par un synthétiseur quantique de tension alternative. La détermination du rapport des deux puissances spectrales obtenues relie la constante de Boltzmann à la constante de Planck. Une analyse détaillée des incertitudes obtenues pour des mesures récentes de bruit montre que la constante de Boltzmann peut être obtenue avec une incertitude relative inférieure à 10×10^{-6}. Un tel niveau d'incertitude rend pertinente la mise en œuvre de cette méthode nouvelle pour mesurer la constante de Boltzmann. ***Pour citer cet article : S. Benz et al., C. R. Physique 10 (2009).***

Keywords: Boltzmann constant; Johnson noise; Josephson arrays; Noise thermometry; Temperature

Mots-clés : Constante de Boltzmann ; Bruit Johnson ; Réseau de jonctions Josephson ; Mesure de bruit thermique ; Température

☆ This work is a contribution of an agency of the U.S. government and is thus not subject to U.S. copyright.

* Corresponding author.
E-mail address: samuel.benz@nist.gov (S. Benz).

1631-0705/$ – see front matter
doi:10.1016/j.crhy.2009.10.008

1. Introduction

Johnson noise describes the fluctuations in voltage and current occurring in all normal-state electrical conductors at a finite temperature [1–3]. These fluctuations are related to the energy dissipation associated with irreversibility and have their origin in the thermally induced motion of conduction electrons. Nyquist's explanation of the noise was the second example of a fundamental result now called the fluctuation–dissipation theorem [3,4] (the first example was Einstein's 1905 explanation of Brownian motion [5]).

Johnson noise is usually characterized by its mean square voltage, conventionally called the noise power. For frequencies below 1 MHz and temperatures above 25 K, it is approximated to better than 1 part in 10^6 by Nyquist's equation,

$$\left\langle V^2 \right\rangle = 4kTR\Delta f \tag{1}$$

where k is Boltzmann's constant, T is the temperature of the resistance R, and Δf is the measurement bandwidth. Johnson–Nyquist noise is often described as a "white noise", since the power spectral density (PSD) $S_{\mathrm{R}} = 4kTR$ is independent of frequency. Because the fluctuation–dissipation theorem is fundamental, Johnson noise thermometers (JNT) are primary thermometers measuring "absolute" thermodynamic temperatures.[1] The most significant measurement challenge of JNT is apparent from (1), namely that the noise voltages are extremely small, $\sim$1.2 nV/Hz$^{1/2}$, for a 100 Ω resistor at the triple point of water. Very-high-performance electronics, cross-correlation measurement techniques, and long averaging times are required to make metrologically useful JNT measurements [11] (for an extensive JNT review see [12]).

Johnson, with his 1928 measurements of the noise, made an interesting first demonstration of noise thermometry by inferring a value of k that agrees with the current value within the uncertainty of his measurements [2]. However, because of the technical difficulties and the non-ideal performance of electronic components, noise thermometry has never achieved uncertainties comparable to those obtained with other primary techniques, especially the various forms of gas thermometry, and has never contributed to a determination of the Boltzmann constant. Nevertheless, with the advent of fast computers and fast, ultra-linear analog-to-digital converters, Johnson noise thermometers are reaching uncertainties of parts in 10^4 and lower, and finding application in temperature-scale comparisons and fixed-point-temperature determinations [12–24].

In conventional JNT systems, one measures the noise power from a sensor at a known temperature (often the triple point of water, which conveniently has a defined temperature in the International System of Units: $T_{\mathrm{w}} \equiv 273.16$ K) and the noise power of a second sensor at the unknown temperature. The temperature is inferred using (1) from the ratio of the measured noise powers and the ratio of the sensing resistances. The most successful JNT technique for the medium- and high-temperature ranges is the switched-input correlator pioneered by Brixy for application in nuclear reactors [14] and is now used routinely for most metrological noise thermometry. It combines the amplifier-noise immunity of cross-correlators, first used by Fink [13], and the gain-instability immunity of the Dicke radiometer [25]. Modern versions eliminate the analog multiplier as a major source of error by digitizing the signals from the two correlator channels and performing the multiplication and averaging functions in software. NIST has adopted the switched digital cross-correlator for its JNT system, but has added a programmable quantized-voltage noise source (QVNS) based on ac-Josephson voltage standards [26–35] as a calculable noise reference. This enables the correlator to compare the power spectral density of the thermal noise of the resistor at the triple point of water with the quantum-mechanically stable synthetic noise generated by the QVNS, and infer a value of k.

In the following sections we describe the experimental apparatus, including the operating principles, and the designs of the QVNS and correlator. The remaining section gives a summary of the uncertainty analysis and recent experimental results.

[1] Other primary thermometers based on electron physics include: all-cryogenic JNTs employing Josephson junctions as voltage-to-frequency converters [6,7]; Coulomb-blockade devices; shot-noise methods; and single-tunnel-junction devices; all having demonstrated relative uncertainties approaching 10^{-3} [8–10].

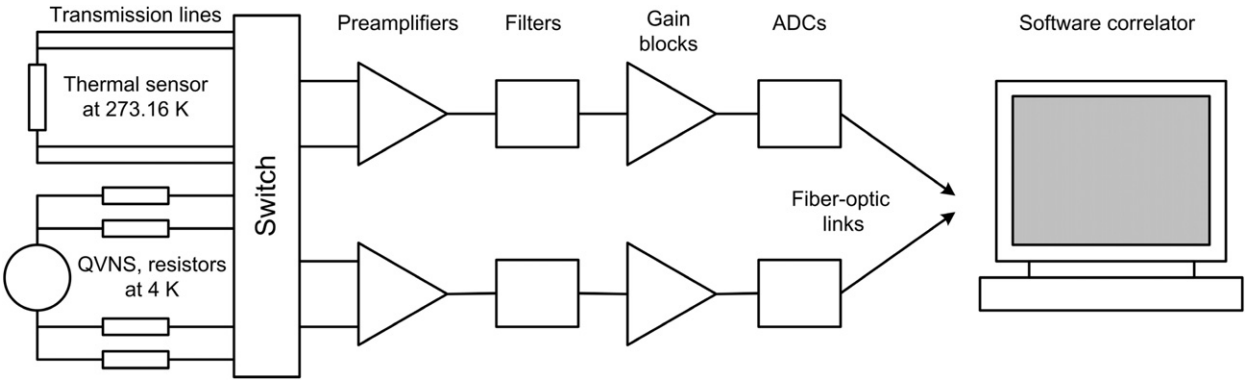

Fig. 1. A simplified schematic diagram of the 2007 NIST Johnson noise thermometer using the quantized-voltage noise source as a synthetic noise reference.

2. Experimental apparatus

2.1. Operating principle

Fig. 1 shows a simplified schematic diagram of the NIST JNT. At the input are the two noise sources. The first is a conventional resistor sensor maintained at the triple point of water, producing Johnson noise with a power spectral density according to (1)

$$S_{\mathrm{R}} = 4kT_{\mathrm{w}}X_{\mathrm{R}}R_{\mathrm{K}} \tag{2}$$

where the sensing resistance is now expressed as the product of the dimensionless ratio X_{R} times the von Klitzing resistance $R_{\mathrm{K}} \equiv h/e^2$ [36], h is Planck's constant, and e is the charge of the electron. The second source produces a synthetic noise with a power spectral density calculable from the various operating parameters of the QVNS and fundamental constants:

$$S_{\mathrm{Q}} = D^2 N_{\mathrm{J}}^2 f_{\mathrm{s}} M / K_{\mathrm{J}}^2 \tag{3}$$

where $K_{\mathrm{J}} \equiv 2e/h$, is the Josephson constant [37], f_{s} is a clock frequency, M is the bit-length of the digital code for the waveform, D is a precisely known parameter that is chosen to closely match the QVNS power spectral density to that of the resistor $S_{\mathrm{Q}} \approx S_{\mathrm{R}}$, and N_{J} is the number of junctions in the Josephson array used to generate the pseudo-noise waveform.

The cross-correlator measures the noise powers of the thermal and QVNS signals. When the bandwidth of the system in the two configurations is the same, the ratio of the noise powers gives the ratio of the power spectral densities $S_{\mathrm{R}}/S_{\mathrm{Q}}$, which is then used to infer

$$k = h\frac{D^2 N_{\mathrm{J}}^2 f_{\mathrm{s}} M}{16 T_{\mathrm{w}} X_{\mathrm{R}}}\frac{S_{\mathrm{R}}}{S_{\mathrm{Q}}} \tag{4}$$

The most significant contribution to the uncertainty in the determination of k is the uncertainty in the noise-power measurements; the uncertainties in Planck's constant, the realization of the triple point of water, and the resistance measurement are practically negligible in comparison (see Section 3 for details).

2.2. The QVNS

The QVNS is a delta-sigma digital-to-analog converter that uses oversampling techniques to produce a programmed sequence of pulses clocked at 5 GHz. With appropriate algorithms and biasing, it produces a pseudo-noise waveform with the desired harmonic content over a 4 MHz baseband, well beyond the nominal 1 MHz bandwidth of the JNT. The primary advantage of the QVNS is that the voltage pulse from each Josephson junction has a quantized area

$$\int V(t)\,\mathrm{d}t = nh/2e \tag{5}$$

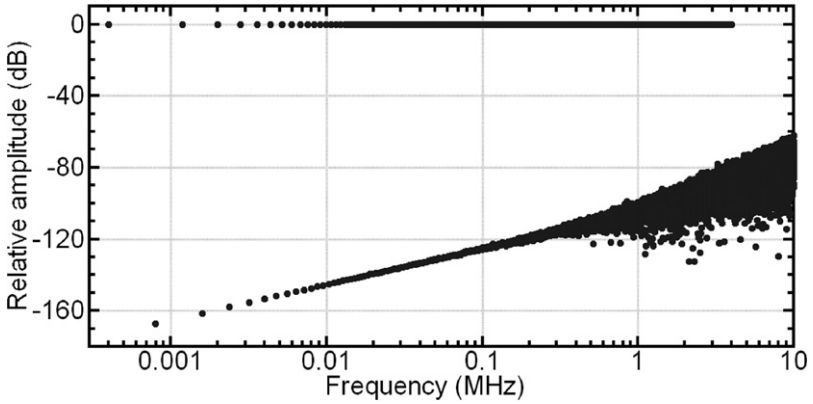

Fig. 2. The first 10 MHz of a typical QVNS spectrum calculated from the code sequence. The upper branch shows the odd harmonics up to 4 MHz ($f_1 \approx 400$ Hz). The lower branch shows the even harmonics up to 4 MHz, and all harmonics above 4 MHz. Below 4 MHz, the amplitudes of the even harmonics are indicative of the voltage targeting (deviation from desired voltage for increasing frequency) of the modulator algorithm for the odd harmonics [28].

where n is an integer (normally $n = 1$ in the NIST QVNS) [28,37]. This enables the synthesized baseband voltage to be calculated exactly from the known sequence of pulses, the clock frequency of the pulse generator, and fundamental physical constants, according to (4).

The synthesis technique underlying the QVNS was originally developed for ac-Josephson voltage standards [26, 27]. However, the low voltages and long integration times of noise thermometry necessitate a specialized QVNS circuit consisting of a pair of symmetric, grounded, lumped arrays, having only a small number of junctions (typically $N_J = 8$ to 256) [30]. Each array is separately biased with a unipolar pulse drive that is clocked at half the 10 GHz sampling frequency, f_s. The QVNS is biased with a continuously recycled digital code that determines the pulse sequence. The code, M bits long, is generated with a delta-sigma analog-to-digital conversion algorithm that is programmed to produce a synthesized waveform with the desired and precisely calculable power spectrum. The spectrum is composed of a series of tones at multiples of the pattern repetition frequency, $f_1 = f_s/M$. The usual JNT waveform is a series of tones at the odd harmonics $f_1, 3f_1, 5f_1, \ldots$, all of the same amplitude but random phase (see Fig. 2). When used to measure k, the rms voltage amplitude V of the tones is adjusted (with the appropriate value of D, see (4)) so that the synthesized waveform's average power spectral density $S_Q = \langle V^2 \rangle / 2f_1$ matches the thermal noise power spectral density, S_R, to within 0.05%. The four impedance-matching resistors terminating the QVNS transmission line are placed in each lead of the transmission line so that they produce only uncorrelated noise, and are maintained at 4 K so that they do not unduly increase the uncorrelated noise in each channel of the correlator.

In addition to providing the link to Planck's constant, the QVNS has important advantages that have enabled significant improvements in the measurements. Unlike a resistor noise source, the QVNS output voltage is inherently independent of its output impedance. This overcomes the matching conflict inherent in conventional Johnson noise thermometers. Now, the thermal and QVNS sources have the same noise power, in order to minimize effects of any amplifier or ADC nonlinearity. An output resistance is chosen to ensure the same frequency responses of the transmission lines between the resistor and QVNS sources and the preamplifiers. This reduces the 'spectral match' error and allows a reduced measurement period due to a greater operating bandwidth [33,35]. The QVNS can also be programmed to produce a variety of different waveforms for diagnostic purposes. In contrast, the noise power and impedance cannot be independently varied in a conventional Johnson noise thermometer, resulting in some degree of mismatch of frequency response and noise power between measurement and reference sensors.

2.3. The correlator

The noise power from the resistor and QVNS are alternately measured by the correlator, depending on the position of the switching network, as indicated in Fig. 1. Each channel of the correlator is composed of a low-noise preamplifier

Table 1
Summary uncertainty budget for a determination of the Boltzmann constant by QVNS noise thermometry. All uncertainties are expressed as relative standard uncertainties in parts in 10^6.

TPW temperature realization		
Source	2007	Soon
Chemical purity	0.15	0.15
Isotopic composition	0.11	0.11
Hydrostatic head	0.18	0.18
Immersion effects	1.8	0.4
Total	1.88	0.58

QVNS waveform		
Source	2007	Soon
Planck's constant	0.05	0.05
Frequency reference	0.001	0.001
Quantization effects	0.1	0.1
Total	0.1	0.1

Resistance measurement		
Source	2007	Soon
Transfer standard	–	0.25
Ratio measurement	–	1
Ac-dc difference	–	0.4
Stability and drift	10	0.25
Total	10	1.13

Noise-power ratio		
Source	2007	Soon
Statistical	19	5.2
Nonlinearity	5	1
Frequency response	5	1
EMI	10	2
Total	22.6	5.8
Grand total	24.8	5.9

and gain blocks with a total gain of about 85 dB, filters to define the bandwidth and prevent aliasing, and a fast ADC. The preamplifier input stage is based on a common-source–common-base FET-bipolar cascode without feedback. This is necessary to meet the demanding requirements of low-input-noise voltage, very-low-input-noise current, low noise-current–noise-voltage correlation, high input resistance, low input capacitance, and a high common-mode rejection ratio [16,35]. The filters are passive *LC*-ladder filters implementing an 11th-order Butterworth response with a cutoff frequency of 600 kHz. The high filter order ensures that the contribution of aliased signals to the measured noise power is negligible.

The ADCs simultaneously sample the signals in each channel for 1 s periods with a 2.08 MHz sampling frequency. The fast Fourier transform (FFT) of the signals is then computed, yielding 1 Hz frequency-resolved FFT bins and a 1.04 MHz Nyquist frequency. To ensure that the QVNS tones are located in a single FFT bin, the ADC clocks are locked to the same frequency reference as the QVNS clock.

The computer carries out a complex frequency-domain cross correlation of the FFT spectra for the two channels to eliminate the amplifier noise voltages, and the autocorrelation for each channel for diagnostic purposes. The computations are carried out in real time, and every 100 s the correlator is switched between the resistor and the QVNS. Once a sufficient number of power spectra have been measured and summed, the ratio of the thermal and QVNS spectra is computed. This removes the filter response from the calculations, ensures equal weighting of all spectral elements in the calculation, and maximizes the correlation bandwidth of the thermometer [34]. Care is required in the implementation of this algorithm in order to avoid a bias caused by the (nonlinear) division calculations operating on the stochastic data (see Section 4 in [34]).

3. Sources of error and uncertainty

Table 1 summarizes the various sources of uncertainty in a JNT Boltzmann-constant determination [35]. Two values are given for many of the terms: our current uncertainty and a projected value indicating what will be readily achievable in the near future. The following subsections discuss some of the contributions to both systematic error and uncertainty, with a focus on the terms that are most significant or where recent significant progress has been made. Most of the sources of uncertainty have been discussed in detail elsewhere, and for further information readers should consult the references.

3.1. Statistical uncertainty

Ideally, the most significant contribution to uncertainty in JNT measurements is the statistical uncertainty arising from the measurement of random processes. The relative uncertainty u_V^2/V^2 in the measurements of the average noise powers $\langle V^2\rangle$ is found from the relative variance [34],

$$\frac{u_{V^2}^2}{\langle V^2\rangle^2} = \frac{1}{2\tau\Delta f_c}\left[\left(1+\frac{S_n}{S}\right)^2 \pm 1\right] \tag{6}$$

where S is the power spectral density of the measured (correlated) noise, S_n is the power spectral density of the (uncorrelated) amplifier noise, τ is the averaging period for the measurement, Δf_c is the correlation bandwidth of the JNT, the + sign refers to the thermal noise-power measurement, and the − sign refers to the QVNS noise-power measurement. The case of (6) for the thermal noise measurement, with the positive sign, is well known. The case of (6) for the QVNS measurement, with the negative sign, arises because the QVNS signal is not truly random; instead it has a constant noise power when integrated over multiples of the code recycle period. Thus, the uncertainty is lower than for the conventional noise-power measurement. Note that the uncertainty in the QVNS measurement is zero when the amplifier noise is zero.

The total measurement period is the sum of the integration periods for the thermal and QVNS measurements; the relative variance in the ratio of the measured power spectral densities is the sum of both versions of (6). The current relative uncertainty for a complete 36-hour measurement is 1.9×10^{-5}. With an integration period of 20 days the uncertainty would be reduced to 5×10^{-6}. To reduce this uncertainty to 2×10^{-6}, would require about 125 days, which was considered to be impractical with our current system.

3.2. Nonlinearity

In order to amplify the ∼35 nV rms signals (∼10 μV total peak voltage for QVNS waveforms with tones up to 4 MHz) to an amplitude appropriate for the ADCs, the gain in each channel of the correlator must be about $\sim 2 \times 10^4$. Inevitably, the nonlinearity in the various amplifier stages, filters, and ADCs accumulates to introduce a significant error in the noise-power measurement. This is mitigated by operating the correlator with the noise-power ratio (PSD ratio S_R/S_Q) close to unity, and hence any systematic errors common to both noise-power measurements have no impact on the measured ratio. For this to occur, several conditions must be satisfied: the synthetic waveform must extend over the entire bandwidth of the system; it must have the same average power spectral density as the thermal noise; and the uncorrelated noises in each channel of the correlator due to the amplifier noise and lead resistances must also be individually matched [33,38]. The uncorrelated-noise match is achieved by inserting low-value (0.1 Ω to 1 Ω) resistors into the leads of the transmission lines.

Some of the causes of nonlinearity are particularly insidious. These include damaged wire, worn connectors, and some solder joints where a small change in the work function of the metal, or a weak insulating barrier, occurs. Ordinarily the potential barriers associated with these phenomena are well below normal signal levels and cause negligible distortion [39]. However, with the very low voltage levels and the multitone waveforms associated with the QVNS, the nonlinearity is apparent. The effects can be difficult to isolate and can impact the measurements directly if they occur in different transmission lines, so are not shared by both signals.

One of the advantages of the QVNS is that it enables *in-situ* detection of nonlinearities in the correlator. For example, nonlinearities acting on the odd-tone spectrum invariably produce even harmonics easily seen in the averaged spectra. At present we see very little dependence of measured noise power on the spectral distribution of the QVNS signal, and estimate that the relative uncertainty due to nonlinearities is about 5×10^{-6}. The electronics nonlinearities are being evaluated, and new waveform synthesis techniques are being investigated that should allow the uncertainty due to nonlinearities to be reduced below 1×10^{-6}. Work is also underway to develop a quantitative spectral test to measure nonlinearity through the whole of the system for both the QVNS and thermal signals [40].

3.3. Frequency response

Because the same correlator is used to measure the noise power for both signals, the measured ratio of the noise powers is independent of the gain and frequency response of the correlator. Frequent (∼100 s) switching between the

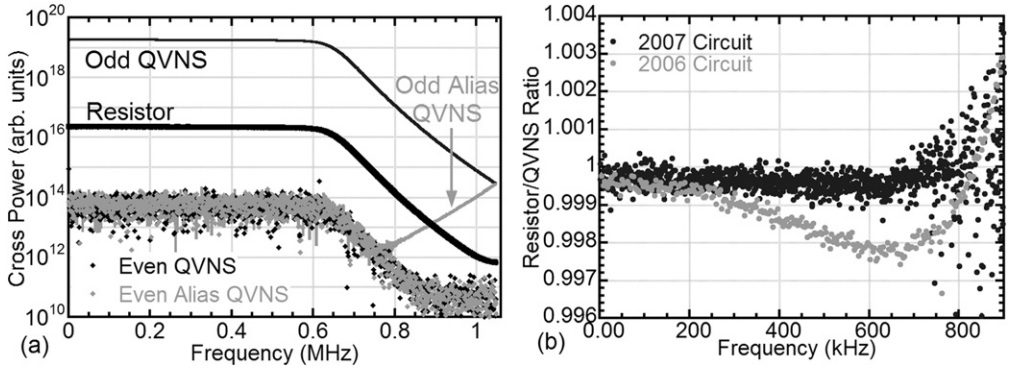

Fig. 3. (a) Measured FFT cross-correlation spectra of resistor noise and QVNS pseudo-noise waveform with only odd-harmonic tones of the 2007 system circuit (passively filtered, eight junctions, $f_1 \approx 400$ Hz). Even QVNS bins show how the uncorrelated noise has decreased well below the PSD after cross-correlating for 7.3 hours. (b) Ratios of the measured power spectra of the resistor Johnson noise and the QVNS pseudo-noise waveform, comparing the frequency response of the 2006 and 2007 systems circuits showing the improvements in frequency response (∼36 h measurement period each) [35].

two sources also minimizes drifts in gain and frequency response. However, because the transmission lines connecting the signals to the correlator are independent, differences in the transfer function of the transmission lines have an impact on the measured noise-power ratio. To ensure a good match, the interactions of the source impedance, lead resistances, inductance, and capacitance must be considered. Departures from an ideal match are easily detected from the ratio of the thermal and QVNS spectra, which should be independent of frequency (see Fig. 3). A carefully chosen combination of impedance-matching resistors and transmission-line lengths ensures a match between the QVNS and resistor transfer functions over a very wide bandwidth. Residual errors in the spectral match have a weak f^2 dependence, which is easily measured and corrected. At present the relative uncertainty due to poor spectral match is estimated to be below 5×10^{-6}, and could probably be reduced to $\sim 1 \times 10^{-6}$, if necessary, by reducing the correlation bandwidth of the thermometer and increasing the integration period.

3.4. Preamplifier noise currents

While the correlator eliminates systematic effects due to the amplifier noise voltages, there remain errors due to the amplifier noise currents and noise-current–noise-voltage correlation. When connected to the thermal noise source, the preamplifier noise currents pass through the sensing resistor and are measured by both channels of the correlator, leading to an error in the noise-power measurement. Correlation between the noise current and the noise voltage is normally purely imaginary, but in combination with the phase shift due to the transmission line capacitance, a second error of a similar magnitude occurs [16]. Both of these errors are relatively small and have an f^2 dependence.

When the correlator is connected to the QVNS, the Josephson array appears as a short circuit, so that both the noise-current and noise-current–noise-voltage errors vanish. The difference in the behavior of two sources therefore leads to a systematic error in the measurement of the noise-power ratio. The effect is eliminated by the same fitting and correction process used to compensate for the f^2-dependent spectral mismatch in the transmission-line frequency response [34].

3.5. Electromagnetic interference (EMI)

EMI is another unavoidable source of error. It is typically intermittent, caused by nearby electrical machinery not associated with the JNT, and for magnetically coupled EMI is difficult to shield. To minimize possible EMI effects, all of the analog electronics and the ADCs are operated from independent battery power supplies, and the ADCs are coupled to the computer via fiber-optic links. While statistical tests on the averaged power spectra can detect stationary single-frequency EMI, in general the tests are not sufficiently powerful to detect all types of EMI [15].

Evidence of the absence of EMI effects in the QVNS measurements is obtained by operating the QVNS so that it generates zero volts. Any non-zero noise-power measurement then indicates the error due to EMI. A similar test can be carried out with the thermal noise source, but this requires a ‘dummy’ sensor of the same impedance and geometric

layout as the real sensor, but generating no correlated noise [21]. Through direct measurements and analysis of the EMI and appropriate placement of the electronics, we anticipate that the EMI uncertainty can be reduced to 2 ppm.

3.6. QVNS waveform

The quantized nature of the voltages produced by the QVNS and its wide bandwidth ensure that the uncertainties arising from the QVNS are small. However, there is still potential for errors, and the most significant error contribution comes from undesired nonquantized signals associated with the current sources biasing the QVNS, such as input–output coupling and bias currents driving inductance in the QVNS circuit. These errors, which fortunately have been undetectable thus far, are most significant at higher frequencies, so they would likely be removed through the fitting analysis.

Another effect that can limit measurement uncertainty is variations in the voltage amplitudes of the synthesized harmonic tones for the QVNS waveform due to digitization or "quantization" noise, which is inherent in the digital-to-analog generation of desired waveform signal from the discrete high-frequency QVNS pulses. The software generating the code for the QVNS shapes this digitization noise and moves most of it to the high-frequency end of the spectrum (see Fig. 2). The resulting error integrated over the bandwidth used in the JNT contributes about 1×10^{-7} to the relative uncertainty. It can be made even lower by choosing a higher-order modulator algorithm and fewer numbers of junctions. Even if this error were currently large enough to limit the measurement uncertainty, the voltage variations are exactly calculable from the waveform, so calculated corrections could be applied to remove this variation from the measurement. Other negligible sources of uncertainty include the uncertainty in the reference frequency and in Planck's constant [41].

3.7. Triple point of water realization

By definition, the triple-point temperature of water is exactly 273.16 K. However, there are uncertainties associated with the realization of the triple point [12,34]. Effects to consider include the isotopic composition of the water, chemical impurities, hydrostatic pressure, and sensor immersion effects (heat leaks). At present, no particular effort has been put into minimizing the effects for which total relative uncertainty is about 2×10^{-6}. Straightforward procedures exist to reduce the uncertainty to 6×10^{-7}.

3.8. Resistance measurement

DC-resistance measurements can be made with relative uncertainties well below 1×10^{-6}. For the JNT, complications arise because we are interested in the real part of the sensor impedance over a very wide range of frequencies. To minimize the frequency dependence of the sensor due to stray inductance, stray capacitance, dielectric loss, and skin effect, a very small thin-film sensor is used. Any remnant reactance is lumped with the transmission-line reactance and corrected by the f^2 fitting and correcting process [23]. At present the uncertainties in the measurement total about 1×10^{-5}. Although care has been taken with the materials used in the transmission line, we have made no particular efforts to reduce the uncertainty. With more work on the traceability chain for the ohm-meter, it can be reduced to about 1×10^{-6}.

4. Conclusion

The addition of the quantized ac-voltage synthesis to Johnson noise thermometry significantly advances the cause of developing a purely electronic high-accuracy primary thermometer. The benefits of the quantized-voltage noise source include improved matching of sensor impedance, enabling a wider bandwidth and reduced measurement period, a simultaneous match of sensor impedance and noise power, enabling a reduction in the effects of nonlinearities, and an ability to synthesize a variety of waveforms suited to diagnosis and assessment of different aspects of the system accuracy. Recent and planned improvements to the QVNS-JNT system and recent experiments suggest that a relative uncertainty of better than 1×10^{-5} will be achieved in the very near future. A measurement at this level of accuracy will provide valuable confirmation for other experiments used to determine the value of the Boltzmann constant.

Acknowledgements

We thank Charlie Burroughs for chip packaging, Ryan Toonen for helpful conversations regarding amplifier nonlinearities, Paul Dresselhaus for QVNS fabrication, computer support and advice, Sae Woo Nam for creative ideas and years of productive collaboration, Dean Ripple for helpful suggestions, and John Martinis for inspiring the QVNS-JNT program.

References

[1] J.B. Johnson, Thermal agitation of electricity in conductors, Nature 119 (1927) 50–51.
[2] J.B. Johnson, Thermal agitation of electricity in conductors, Phys. Rev. 32 (1928) 97–109.
[3] H. Nyquist, Thermal agitation of electric charge in conductors, Phys. Rev. 32 (1928) 110–113.
[4] H.B. Callen, T.A. Welton, Irreversibility and generalized noise, Phys. Rev. 83 (1951) 34–40.
[5] A. Einstein, On the motion—required by the molecular kinetic theory of heat—of small particles suspended in a stationary liquid, Annalen der Physik 17 (1905) 549–560.
[6] R.J. Soulen, R.L. Rusby, D. Van Vechten, A self-calibrating rhodium–iron resistive SQUID thermometer for the range below 0.5 K, J. Low Temp. Phys. 40 (1980) 553–569.
[7] J.C. Gallop, B.W. Petley, Josephson noise thermometry with HTS devices, IEEE Trans. Instrum. Meas. 44 (1995) 234–237.
[8] J.P. Pekola, K.P. Hirvi, J.P. Kauppinen, M.A. Paalanen, Thermometry of arrays of tunnel junctions, Phys. Rev. Lett. 73 (1994) 2903.
[9] L. Spietz, K.W. Lehnert, I. Siddiqi, R.J. Schoelkopf, Primary electronic thermometry using the shot noise of a tunnel junction, Science 300 (2003) 1929–1932.
[10] J.P. Pekola, T. Holmqvist, M. Meschke, Primary tunnel junction thermometry, Phys. Rev. Lett. 101 (2008) 206801-1–4.
[11] R.A. Webb, R.P. Giffard, J.C. Wheatley, Noise thermometry at ultralow temperatures, J. Low Temp. Phys. 13 (1973) 383–429.
[12] D.R. White, R. Galleano, A. Actis, H. Brixy, M. De Groot, J. Dubbeldam, A.L. Reesink, F. Edler, H. Sakurai, R.L. Shepard, J.C. Gallop, The status of Johnson noise thermometry, Metrologia 33 (1996) 325–335.
[13] H.J. Fink, A new absolute noise thermometer at low temperatures, Can. J. Phys. 37 (1959) 1397–1406.
[14] H. Brixy, R. Hecker, J. Oehmen, K.F. Rittinghaus, W. Setiawan, E. Zimmermann, Noise thermometry for industrial and metrological applications at KFA Jülich, in: J.F. Schooley (Ed.), Temperature, Its Measurement and Control in Science and Industry, vol. 6, Am. Inst. Phys., New York, 1992, pp. 993–996.
[15] R. Willink, D.R. White, Detection of corruption in Gaussian processes with application to noise thermometry, Metrologia 35 (1998) 787–798.
[16] D.R. White, E. Zimmermann, Preamplifier limitations on the accuracy of Johnson noise thermometers, Metrologia 37 (2000) 11–23.
[17] D.R. White, R.S. Mason, P. Saunders, Progress towards a determination of the indium freezing point by Johnson noise thermometry, in: B. Fellmuth, J. Seidel, G. Scholz (Eds.), Proceedings of TEMPMEKO 2001, VDE Verlag, Berlin, 2001, pp. 129–134.
[18] H. Howener, Noise Thermometry in Nuclear Power Plants, KFA, Jülich GmbH, JUL-2107, 1986.
[19] H. Saleh, E. Zimmerman, G. Brandenburg, H. Halling, Efficient FPGQ-based multistage two-path decimation filter for noise thermometer, in: Proceedings of ICM 2001, IEEE Catalog No. 01EX481, Rabat, Morocco, 2001, pp. 161–164.
[20] M. Frigo, S.G. Johnson, FFTW, Massachusetts Institute of Technology, 2003, http://www.fftw.org.
[21] D.R. White, R.S. Mason, An EMI test for Johnson noise thermometry, in: D. Zvizdic, L.G. Bermanec, T. Stasic, T. Veliki (Eds.), Proceedings of TEMPMEKO 2004, Faculty of Mechanical Eng. and Naval Arch., Zagreb, 2004, pp. 485–490.
[22] J.T. Zhang, S.Q. Xue, A noise thermometry investigation of the melting point of gallium at the NIM, Metrologia 43 (2006) 273–277.
[23] W.L. Tew, J.R. Labenski, S.W. Nam, S.P. Benz, P.D. Dresselhaus, C.J. Burroughs, Johnson noise thermometry near the zinc freezing point using resistance-based scaling, Int. J. Thermophys. 28 (2007) 629–645.
[24] J.R. Labenski, W.L. Tew, S.W. Nam, S.P. Benz, P.D. Dresselhaus, C.J. Burroughs, A determination of the ratio of the zinc freezing point to the tin freezing point by noise thermometry, in: Proceedings of TEMPMEKO 2007, Int. J. Thermophys. 29 (2008) 1–17.
[25] R.H. Dicke, The measurement of thermal radiation at microwave frequencies, Rev. Sci. Instrum. 17 (1964) 268–275.
[26] S.P. Benz, C.A. Hamilton, A pulse-driven programmable Josephson voltage standard, Appl. Phys. Lett. 68 (1996) 3171–3173.
[27] S.P. Benz, C.A. Hamilton, C.J. Burroughs, T.E. Harvey, L.A. Christian, J.X. Przybysz, Pulse-driven Josephson digital/analog converter, IEEE Trans. Appl. Supercond. 8 (1998) 42–47.
[28] S.P. Benz, J.M. Martinis, S.W. Nam, W.L. Tew, D.R. White, A new approach to Johnson noise thermometry using a Josephson quantized voltage source for calibration, in: B. Fellmuth, J. Seidel, G. Scholz (Eds.), Proceedings of TEMPMEKO 2001, the 8th International Symposium on Temperature and Thermal Measurements in Industry and Science, VDE Verlag, Berlin, April 2002, pp. 37–44.
[29] S.W. Nam, S.P. Benz, P.D. Dresselhaus, W.L. Tew, D.R. White, J.M. Martinis, Johnson noise thermometry measurements using a quantum voltage noise source for calibration, IEEE Trans. Instrum. Meas. 52 (2003) 550–553.
[30] S.P. Benz, P.D. Dresselhaus, J.M. Martinis, An ac Josephson source for Johnson noise thermometry, IEEE Trans. Instrum. Meas. 52 (2003) 545–549.
[31] S.W. Nam, S.P. Benz, P.D. Dresselhaus, C.J. Burroughs, W.L. Tew, D.R. White, J.M. Martinis, Progress on Johnson noise thermometry using a quantum voltage noise source for calibration, IEEE Trans. Instrum. Meas. 54 (2005) 653–657.
[32] S.W. Nam, S.P. Benz, J.M. Martinis, P.D. Dresselhaus, W.L. Tew, D.R. White, A ratiometric method for Johnson noise thermometry using a quantized voltage noise source, in: D.C. Ripple (Ed.), Temperature: Its Measurement and Control In Science and Industry, vol. 7, American Institute of Physics, Melville, New York, 2003, pp. 37–42.
[33] D.R. White, S.P. Benz, Constraints on a synthetic-noise source for Johnson noise thermometry, Metrologia 45 (2008) 93–101.

[34] D.R. White, S.P. Benz, J.R. Labenski, S.W. Nam, J.F. Qu, H. Rogalla, W.L. Tew, Measurement time and statistics for a noise thermometer with a synthetic-noise reference, Metrologia 45 (2008) 395–405.
[35] S.P. Benz, H. Rogalla, D.R. White, J.F. Qu, P.D. Dresselhaus, W.L. Tew, S.W. Nam, Improvements in the NIST Johnson noise thermometry system, IEEE Trans. Inst. Meas. 58 (2009) 884–890.
[36] K. von Klitzing, G. Dorda, M. Pepper, New method for high-accuracy determination of the fine-structure constant based on quantized Hall resistance, Phys. Rev. Lett. 45 (1980) 494–497.
[37] B.D. Josephson, Possible new effects in superconductive tunneling, Phys. Lett. 1 (1962) 251–253.
[38] L. Storm, Measurement of small noise signals with a correlator and noise thermometry at low temperatures, Z. Angew. Phys. 6 (1969) 331–333.
[39] E. Takano, Contact current distortion due to tunnel effect, in: Proceedings of the Forty-Fifth IEEE Holm Conference on Electrical Contacts, 4–6 Oct. 1999, Pittsburgh, PA, USA, pp. 136–140.
[40] Jifeng Qu, S.P. Benz, H. Rogalla, D.R. White, Reduced nonlinearities and improved temperature measurements for the NIST Johnson noise thermometer, Metrologia 46 (2009) 512–524.
[41] P.J. Mohr, B.N. Taylor, D.B. Newell, CODATA recommended values of the fundamental physical constants: 2006, Rev. Mod. Phys. 80 (2008) 633–730.